

motor behaviors. The first was the forward optomotor response (OMR)^{1,2}, in which swimming is elicited by visual gratings moving in the tail-to-head direction. In our system, the OMR during light-sheet scanning was comparable to the OMR without the presence of the light sheets (Fig. 1c). We defined an optomotor index as the difference in swimming strength during and before stimulus presentation. This index was significantly positive in all fish tested, with or without the laser ($P = 0.031$ with laser and $P = 0.031$ without it; two-sided sign test, $n = 6$ fish), and its magnitude was comparable between the two conditions (optomotor index: 0.67 ± 0.13 with the laser and 0.72 ± 0.067 without it, mean \pm s.d.; $P = 0.22$, two-sided paired sign test).

We also tested a more complex behavior: fictive motor adaptation, where the fish adapts its motor output to the strength of visual feedback in a closed-loop paradigm¹. Again, the behavior was comparable with and without the light sheets (Fig. 1d). We defined a gain adaptation index as the ratio of swimming during low gain and high gain. This index was significantly greater than 1 in all fish tested ($P = 0.0078$ with laser and $P = 0.0078$ without it; two-sided sign test, $n = 8$). Its magnitude was also comparable between the two conditions (gain adaptation index: 2.08 ± 0.57 with the laser and 1.91 ± 0.47 without it, mean \pm s.d.; $P = 0.29$, two-sided paired sign test).

The preservation of the OMR and gain adaptation indicates that whole-brain light-sheet imaging is compatible with fictive virtual-reality assays and can be used to interrogate whole-brain activity during visuomotor behavior. As an example, we measured whole-brain activity during the OMR in a 6 d.p.f. transgenic zebrafish expressing the genetically encoded calcium indicator GCaMP6s⁸ under the pan-neuronal *elavl3* promoter (Supplementary Note). Light-sheet imaging captures stimulus and motor-dependent patterns of whole-brain neural activity (Fig. 1e and Supplementary Video 1) with single-cell resolution across most of the brain (Fig. 1f,g and Supplementary Note). Cells and neuropil distributed across the brain showed activity during the optomotor response. We additionally assessed resolution using a fish with nuclear-localized (histone H2B fusion) expression of GCaMP6s (Supplementary Note, Supplementary Figs. 2 and 3, and Supplementary Video 2). Fish lines and DNA constructs for *elavl3:GCaMP6s* and *elavl3:H2B-GCaMP6s* are available upon request.

We presented a system for monitoring neural activity, at the cellular level, across the entire brain of the larval zebrafish during visuomotor behavior. Resources associated with this work, including sample data and analysis resources, are available via <http://research.janelia.org/zebrafish/>. This system, in combination with large-scale data analysis methods described in a companion paper⁹, holds promise for advancing the understanding of how activity in large networks of neurons underlies behavior.

Note: Any Supplementary Information and Source Data files are available in the online version of the paper (doi:10.1038/nmeth.3040).

ACKNOWLEDGMENTS

We thank M. Coleman for writing the light-sheet microscope control software Zebrascope and for continuing support; B. Coop and T. Tabachnik for their help with hardware design; S. Narayan for help with experiments; ID&F engineers for providing help on hardware components; J. Cox, R. Larson, J. Barber, B. Brandenburg and other vivarium staff for fish husbandry; G. Ceric, V. Samalam, K. Carlisle and R. Lines for assistance with the high-performance computer cluster; D.G.C. Hildebrand and M. Koyama for discussions; and V. Jayaraman, M. Reiser and G. Murphy for comments on the manuscript. This work was supported by the Howard Hughes Medical Institute.

AUTHOR CONTRIBUTIONS

M.B.A., P.J.K. and N.V. conceived of the project. M.B.A., P.J.K. and N.V. designed the experimental setup with contributions from D.V.B.; N.V. and M.B.A. built it. Y.M., T.K. and N.V. performed the experiments. N.V., T.K. and M.B.A. wrote the behavior software. J.F. and N.V. performed the imaging analysis. C.-T.Y. and L.L.L. developed the transgenic zebrafish. M.B.A., J.F. and N.V. wrote the paper with contributions from all authors.

COMPETING FINANCIAL INTERESTS

The authors declare no competing financial interests.

Nikita Vladimirov, Yu Mu, Takashi Kawashima, Davis V Bennett, Chao-Tsung Yang, Loren L Looger, Philipp J Keller, Jeremy Freeman & Misha B Ahrens

Janelia Farm Research Campus, Howard Hughes Medical Institute, Ashburn, Virginia, USA.

e-mail: ahrensm@janelia.hhmi.org

PUBLISHED ONLINE 27 JULY 2014; DOI:10.1038/NMETH.3040

- Ahrens, M.B. *et al. Nature* **485**, 471–477 (2012).
- Portugues, R., Feierstein, C.E., Engert, F. & Orger, M.B. *Neuron* **81**, 1328–1343 (2014).
- Ahrens, M.B., Orger, M.B., Robson, D.N., Li, J.M. & Keller, P.J. *Nat. Methods* **10**, 413–420 (2013).
- Panier, T. *et al. Front. Neural Circuits* **7**, 65 (2013).
- Broxton, M. *et al. Opt. Express* **21**, 25418–25439 (2013).
- Quirin, S., Jackson, J., Peterka, D.S. & Yuste, R. *Front. Neural Circuits* **8**, 29 (2014).
- Prevedel, R. *et al. Nat. Methods* **11**, 727–730 (2014).
- Chen, T.-W. *et al. Nature* **499**, 295–300 (2013).
- Freeman, J. *et al. Nat. Methods* doi:10.1038/nmeth.3041 (27 July 2014).

Guided visual exploration of genomic stratifications in cancer

To the Editor: Cancer is a heterogeneous disease, and molecular profiling of tumors from large cohorts has enabled characterization of new tumor subtypes. This is a prerequisite for improving personalized treatment and ultimately achieving better patient outcomes. Potential tumor subtypes can be identified with methods such as unsupervised clustering¹ or network-based stratification², which assign patients to sets based on high-dimensional molecular profiles. Detailed characterization of identified sets and their interpretation, however, remain a time-consuming exploratory process.

To address these challenges, we combined ‘StratomeX’³, an interactive visualization tool that is freely available at <http://www.caleydo.org/>, with exploration tools to efficiently compare multiple patient stratifications, to correlate patient sets with clinical information or genomic alterations and to view the differences between molecular profiles across patient sets. Although we focus on cancer genomics here, StratomeX can also be applied in other disease cohorts.

Thousands of patient stratifications can be derived from large cancer genomics datasets. This space of patient stratifications—which we call the ‘stratome’—contains stratifications based on, for example, clustering of mRNA, microRNA or protein expression matrices; the mutation or copy number status of genes; or on clinical variables. Owing to the size of the stratome and the heterogeneity of the underlying datasets, integration of computational and visual approaches is indispensable to the analyst in identifying biologically or clinically meaningful stratifications as well as clinical parameters and pathways that together provide a comprehensive view of each patient set.

StratomeX complements the network viewers, heat maps and genome browsers typically used in cancer genomics⁴

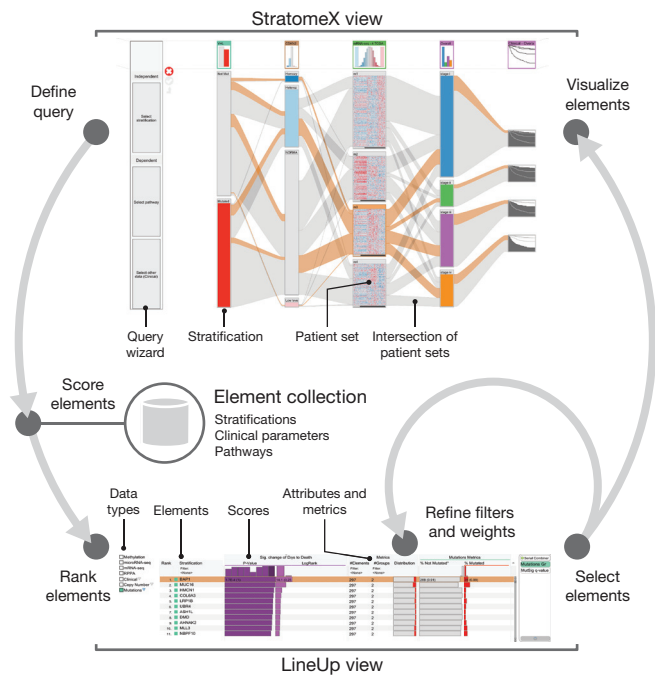


Figure 1 | Seamless integration of visual and computational components in the extended StratomeX tool. In the StratomeX view (top) columns represent different stratifications, each of which are divided into patient sets, and the bands between the columns represent the patients in the intersection of the connected sets. The wider the bands, the higher the correlation between patient sets. Orange bands indicate selected patients. The results of queries are lists of elements ranked by a score, which are shown in the LineUp view (bottom). Elements selected in the LineUp view are immediately visualized in the StratomeX view, enabling analysts to rapidly explore the results of queries.

(Supplementary Discussion and Supplementary Table 1). To visualize the relationships between multiple patient stratifications as well as other data (Fig. 1 and Supplementary Fig. 1), stratifications are represented as columns of stacked blocks where each block corresponds to a patient set. Blocks contain visualizations of the data associated with those patients, such as heat maps, pathway maps overlaid with expression data or survival plots (Supplementary Fig. 2). Bands connecting the blocks show the pairwise overlap of sets in adjacent stratifications, with the width of the bands representing the size of the overlap relative to the size of the patient sets (Supplementary Fig. 3). This visualization is an efficient tool to confirm hypotheses about gene functions or subtypes defined by molecular profiles.

StratomeX also integrates a computational framework for query-based guided exploration of the stratome directly into the visualization (Fig. 1), which enables discovery of novel relationships between patient sets and efficient generation and refinement of hypotheses about tumor subtypes. A ‘query wizard’ provides step-by-step instructions (Supplementary Figs. 1 and 4) for defining queries, and a range of computational methods are used to generate

rankings (Supplementary Methods). The queries yield a score for each stratification, for example, based on their overlap with a particular patient set or based on their overall similarity to a selected stratification. Furthermore, the analyst can query the collection for stratifications that contain patient sets that exhibit differences in survival or differential regulation of pathways. We use ‘LineUp’⁵, a multi-attribute ranking technique, to visualize the results of these queries and to show which stratifications or pathways score highly (Fig. 1 and Supplementary Fig. 5). The tight integration between the StratomeX and LineUp views, as well as the dynamic computation of scores, is essential for rapid identification of meaningful relationships between stratifications, clinical parameters and pathways.

We demonstrate the effectiveness of StratomeX in a case study (Supplementary Note, Supplementary Figs. 6–18, Supplementary Tables 2 and 3, Supplementary Data 1–4 and Supplementary Video 1) in which we explored molecular and clinical data to characterize tumor subtypes in a cohort of over 400 clear cell renal cell carcinoma cases reported by The Cancer Genome Atlas consortium⁶.

Note: Any Supplementary Information and Source Data files are available in the online version of the paper (doi:10.1038/nmeth.3073).

ACKNOWLEDGEMENTS

This work was supported by US National Institutes of Health (U24 CA144025, U24 CA143845 and K99 HG007583), the Austrian Science Fund (J 3437-N15, P 22902), and the Air Force Research Laboratory and Defense Advanced Research Projects Agency grant FA8750-12-C-0300.

AUTHOR CONTRIBUTIONS

M.S., A.L. and N.G. jointly conceived the project and designed the methods. M.S., A.L. and N.G. wrote the manuscript with contributions from S.G. and guidance by P.J.P., H.P. and D.S. M.S. and A.L. led the implementation of the software. S.G. and C.P. contributed to the design and implementation. P.J.P. and N.G. developed requirements and use cases, and oversaw the project.

COMPETING FINANCIAL INTERESTS

The authors declare no competing financial interests.

Marc Streit^{1,6}, **Alexander Lex**^{2,6}, **Samuel Gatzl**¹, **Christian Partl**³, **Dieter Schmalstieg**³, **Hanspeter Pfister**², **Peter J Park**⁴ & **Nils Gehlenborg**^{4,5}

¹Institute of Computer Graphics, Johannes Kepler University Linz, Linz, Austria.

²School of Engineering and Applied Sciences, Harvard University, Cambridge, Massachusetts, USA.

³Institute for Computer Graphics and Vision, Graz University of Technology, Graz, Austria.

⁴Center for Biomedical Informatics, Harvard Medical School, Boston, Massachusetts, USA.

⁵Cancer Program, Broad Institute of Massachusetts Institute of Technology and Harvard, Cambridge, Massachusetts, USA.

⁶These authors contributed equally to this work.

e-mail: nils@hms.harvard.edu or peter_park@hms.harvard.edu

- Verhaak, R. *et al. Cancer Cell* **17**, 98–110 (2010).
- Hofree, M., Shen, J. P., Carter, H., Gross, A. & Ideker, T. *Nat. Methods* **10**, 1108–1115 (2013).
- Lex, A. *et al. Computer Graphics Forum* **31**, 1175–1184 (2012).
- Schroeder, M.P., Gonzalez-Perez, A. & Lopez-Bigas, N. *Genome Med.* **5**, 9 (2013).
- Gatzl, S., Lex, A., Gehlenborg, N., Pfister, H.P. & Streit, M. *IEEE Trans. Visualization Computer Graphics* **19**, 2277–2286 (2013).
- The Cancer Genome Atlas Research Network. *Nature* **499**, 43–49 (2013).